Geochimica et Cosmochimica Acta Vol. 56, pp. 2605–2617

0016-7037/92/$5.00 + .00

An equation of state for the CH_4-CO_2-H_2O system: I. Pure systems from 0 to 1000°C and 0 to 8000 bar

ZHENHAO DUAN, NANCY MØLLER, and JOHN H. WEARE
Department of Chemistry, 0340, University of California, San Diego, La Jolla, CA 92093-0340, USA

(*Received August* 27, 1991; *accepted in revised form April* 23, 1992)

Abstract—An equation of state (EOS) for the CH_4-CO_2-H_2O system covering a wide T-P range has been developed. In this article the new EOS is presented and applied to the pure endmembers. The equation is similar to that of LEE and KESLER (1975) and contains fifteen parameters. It is used with a mixing rule in the following article to provide a thermodynamic model for the mixed system. Though the parameters are evaluated from the PVT data in the temperature range from 0 to 450°C for CH_4, from 0 to 1000°C for CO_2 and H_2O, and for pressures from 0 to 3500 bar, comparison of this EOS with a large amount of experimental data in the pure systems indicates that predictions for temperatures and pressures from 0 to 1000°C and 0 to 8000 bar (or slightly above) are very nearly within experimental uncertainty. The EOS can describe both the gas and the liquid phases of the endmember systems with similar accuracy. Fugacity coefficients are derived and compiled. In this paper mixing is considered using ideal mixing based on the endmember fugacities (Amagat's rule). It is shown that such an approach leads to quite accurate predictions for high temperatures and low pressures.

NOTATION

R = universal constant 0.08314467 bar · $dm^3\ K^{-1}\ mol^{-1}$
T = temperature in °K
P = pressure in bar
V = molar volume in liter or dm^3/mol
ρ = density in mol/dm^3
x = composition
Z = PV/RT (compressibility factor)
G = Gibbs free energy
ΔZ = standard deviation in compressibility factor
$= \sqrt{\dfrac{\sum (Z_{cal} - Z_{exp})^2/Z_{exp}}{n}}$
B, C, D, E, F = virial coefficients as defined in Eqn. (2)
x = mole fraction of components in mixture
μ = chemical potential
f = fugacity
$\phi = f/P$ = fugacity coefficient
n = # of observations or # of components in mixture
m = # of phases
a_i = parameters as given in Table 3 and used in Eqn. (2)
α, β, γ = parameters as given in Table 3 and used in Eqn. (2)

Superscripts

p = pure
M = mixture
id = ideal substances or ideal mixing
α, β = phase identification
0 = standard state

Subscripts

pc = pseudocritical
ex = excess
c = critical condition
r = reduced properties
i, j, k = component identification
T = temperature
P = pressure

I. INTRODUCTION

EQUATIONS OF STATE (EOS) have wide applications in the study of fluid inclusions (e.g., RAMBOZ et al., 1985; VROLIJK, 1987; LIRA and RIPLEY, 1990), diagenesis (CAPUANO, 1990), devolatilization equilibria (JACOBS and KERRICK, 1981b), and solubility of gases in aqueous solutions (CARROLL and MATHER, 1989; DUAN et al., 1992). Many natural fluids fall in the system H_2O-CH_4-CO_2-N_2-salt-SiO_2 (ROEDDER, 1972; HENDEL and HOLLISTER, 1981; SCHMIDT, 1973; SCHMIDT and MCDONALD, 1979; RUMBLE et al., 1982). Among these species, H_2O, CH_4 and CO_2 are found far more frequently. Since VAN DER WAALS (1873), hundreds of equations of state have been published. Some of them are general (e.g., REDLICH and KWONG, 1949; LEE and KESLER, 1975). Others are specifically parameterized for the system or the subsystems of H_2O-CH_4-CO_2 (ANGUS et al., 1976, 1978; KERRICK and JACOBS, 1981; JACOBS and KERRICK 1981a; BOWERS and HELGESON, 1983; SAXENA and FEI, 1987). As will be seen in the following sections and the next article, while some of these EOS are highly accurate in some ranges of temperature and pressure, none can predict phase equilibria in water-containing systems with sufficient accuracy.

While not displaying very complicated chemistry as compared, for example, to aqueous solutions (WEARE, 1987), mixtures in this system are difficult to describe over the large ranges of temperature and pressure where the model will find application (CHOU and WILLIAMS, 1977; JACOBS and KERRICK, 1981b; VAN DEN KERKHOF, 1990). At high temperatures and pressures the endmembers show large deviations from ideal behavior, although ideal mixing may provide an adequate estimate of the free energy of mixtures in some cases (see Section IV). At lower temperatures the system may show multiple phases or form solid phases (VAN DEN KERKHOF, 1990). Describing both phase equilibrium and pressure-volume-temperature (PVT) properties over a large range with one equation is a considerable challenge. The purpose of the EOS in this study is to predict both PVT and liquid-vapor phase equilibria from 0 to 1000°C and from 0 to 8000 bar for pure systems, and from 50 to 1000°C and from 0 to 1000 bar for mixtures.

An EOS is generally chosen on the basis of its ability to describe the system with the desired accuracy over the range of the data used in the parameter adjustment and to extrapolate beyond the experimental range. It is usually based on various forms justified by approximate theoretical results (e.g., the virial equation, hard sphere gas results, etc.). However, these justifications are only qualitative. In all cases accurate representations must contain parameters which are evaluated from experimental data. If properly chosen an EOS provides a method of interpolating data from simple to more complex systems (i.e., from binary to ternary and higher mixing) and, with caution, of extrapolating to *T* and *P* ranges outside the range of the data set used in the parameterization. Generally, because of the required accuracy, extrapolations beyond the data set should be checked carefully. For example, we will show by direct comparison with data that our EOS will provide extrapolations well beyond the range of parameterization.

In the following section we discuss our choice of EOS and its application to the pure endmember systems. Predictions of the pure system behavior are almost within experimental error over the entire range of the data. In Section III the equations required to calculate fugacities are given. In the final section the EOS is extrapolated to high *T* and *P* and the results are compared to the limited experimental data. Ideal mixing is discussed and it is shown that this approximation provides sufficient accuracy for applications at high temperatures and low pressures. The mixing rule and mixtures are discussed in the next article.

II. DESCRIPTION OF THE EQUATIONS FOR PURE SYSTEMS

The choice of EOS is dependent on the range of the data set and the accuracy of reproduction of the experimental measurements that are desired. Since our final purpose is to calculate the thermodynamic properties of mixed systems, we choose a form that is general enough to describe all the systems of interest with similar accuracy. Because application to phase equilibria is envisioned, integration of the EOS to obtain the free energy must be convenient. To treat phase transitions, it is necessary to represent both the gaseous and the liquid states of the system with a single equation.

A number of EOS have been suggested in the literature (see Appendix for a brief description of those tested here). Some of them represent the pure system data quite accurately over part of the range of interest, but have not been generalized to treat mixing. Other forms have been generalized to

Table 1. PTV Data for CH_4, CO_2 and H_2O

System	Authors	Temperature (°C)	P(bar)	# of measurements
CH_4	Douslin et al.	0-350	16-400	240
	Olds et al.	20-250	0-700	294
	Deffet & Ficks	50-150	0-3000	156
	Michels & Nederbragt	0-150	400	68
	Keyes & Burks	0-200	30-250	40
	Schamp et al.	0-150	18-250	118
	Tsiklis & Linshits	50-400	8500	70
	Robertson & Babb	35-200	1000-2500	26
	Din	0-150	1-1000	55
	Kvalnes & Gaddy	0-200	1-1000	44
	Francesconi	150-450	300-2800	89
CO_2	Michels et al.	0-150	16-3000	329
	Vukalovich et al.	0-750	1-600	493
	Kennedy	0-1000	25-1400	2120
	Sass et al.	50-100	8-500	47
	McCormack et al.	0-600	1-50	52
	Kirillin et al.	0-35	16-500	39
	Juza et al.	50-450	700-4000	82
	Greenwood	450-800	50-500	79
	Reamer et al.	38-238	14-700	142
H_2O	Burnham et al.	20-1000	100-8900	4280
	Greenwood	450-800	50-500	79
	Haar et al.	0-374.1	0-218.3	330
	D'Ans et al.	0-800	1-1000	580

Table 2 The Critical Properties of CH_4, CO_2 and H_2O

Components	CH_4	CO_2	H_2O
T_c(°C)	-82.55	31.05	374.1
P_c(bar)	46.41	73.825	221.19

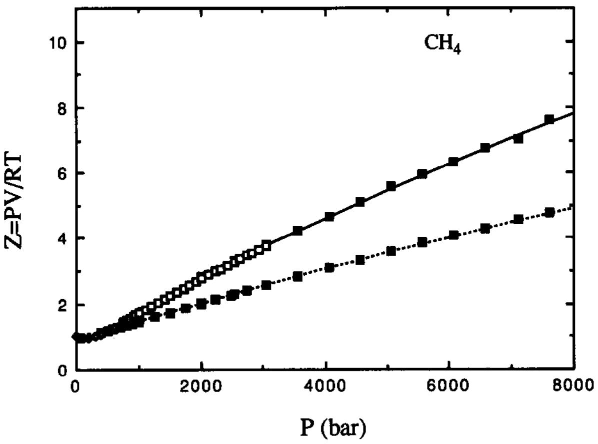

FIG. 1. Comparison of the experimental compressibility factor of CH_4 with prediction of Eqn. (1). The data for pressures above 3500 bar were not included in the parameterization. Solid line = 100°C; dashed line = 400°C. Symbols: ◘, FRANCESCONI (1978); ◆, DIN (1961); ■, TSIKLIS and LINSHITS (1967); □, DEFFET and FICKS (1965).

treat mixtures, but do not accurately represent the PVT relations over the wide range of temperatures and pressures of interest. None of these can predict phase equilibrium in water-containing mixtures.

A useful general discussion of EOS has been given by WALAS (1985). This work recommends the REDLICH and KWONG equation (1949; hereinafter RK) and the LEE and KESLER equation (1975; hereinafter LK) for general purposes. The International Union of Pure and Applied Chemistry (IUPAC) has also suggested forms (ANGUS et al., 1978, for CH_4; 1976 for CO_2). A new EOS for vapor H_2O has been published by NISHIUMI (1980b, for H_2O). Of importance to the geochemical problems of interest here is the work of KERRICK and JACOBS (1981; hereinafter KJ) and JACOBS and KERRICK (1981a; hereinafter JK). They also proposed a model for the CH_4-CO_2-H_2O system. As we will show in the following article, the predictions of this equation are adequate (but not as accurate as the EOS presented here) for the high temperature and pressure range of application to problems in metamorphism. However, at the lower pressures and temperatures relevant to studies of diagenesis and fluid inclusions, the KJ equation does not have the correct behavior to describe the liquid phase.

After extensive comparisons of the available EOS with PVT data it became apparent that in order to describe the system over the range of pressure and temperature of interest and in both the liquid and gas phases, a new EOS would be necessary. In order to proceed we tested a number of forms. Among these were the RK EOS as modified by KERRICK and JACOBS (1981), the BENEDICT, WEBB, RUBIN equation (1940; hereinafter BRW; the BWR equation has been widely used for hydrocarbons and organic fluids; BENDER, 1970; NISHIUMI, 1980a, 1980b), and the LK EOS. None of these were able to provide the required accuracy. Finally a modification of the LK form was chosen.

$$Z = \frac{PV}{RT} = \frac{P_r V_r}{T_r} = 1 + \frac{B}{V_r} + \frac{C}{V_r^2} + \frac{D}{V_r^4} + \frac{E}{V_r^5} + \frac{F}{V_r^2}\left(\beta + \frac{\gamma}{V_r^2}\right)\exp\left(-\frac{\gamma}{V_r^2}\right), \quad (1)$$

where

$$B = a_1 + \frac{a_2}{T_r^2} + \frac{a_3}{T_r^3} \quad (2a)$$

Table 3. EOS Parameters for CH_4, CO_2 and H_2O

parameters	CH_4	CO_2	H_2O
a_1	8.72553928D-02	8.99288497D-02	8.64449220D-02
a_2	-7.52599476D-01	-4.94783127D-01	-3.96918955D-01
a_3	3.75419887D-01	4.77922245D-02	-5.73334886D-02
a_4	1.07291342D-02	1.03808883D-02	-2.93893000D-04
a_5	5.49626360D-03	-2.82516861D-02	-4.15775512D-03
a_6	-1.84772802D-02	9.49887563D-02	1.99496791D-02
a_7	3.18993183D-04	5.20600880D-04	1.18901426D-04
a_8	2.11079375D-04	-2.93540971D-04	1.55212063D-04
a_9	2.01682801D-05	-1.77265112D-03	-1.06855859D-04
a_{10}	-1.65606189D-05	-2.51101973D-05	-4.93197687D-06
a_{11}	1.19614546D-04	8.93353441D-05	-2.73739155D-06
a_{12}	-1.08087289D-04	7.88998563D-05	2.65571238D-06
α	4.48262295D-02	-1.66727022D-02	8.96079018D-03
β	7.53970000D-01	1.39800000D+00	4.02000000D+00
γ	7.71670000D-02	2.96000000D-02	2.57000000D-02

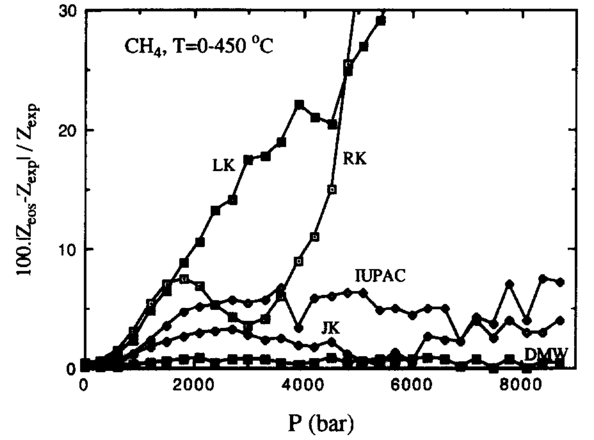

FIG. 2. The deviation of the experimental compressibility factor of CH_4 from predictions of EOS. $\frac{|Z_{cal} - Z_{exp}|}{Z_{exp}}$ is average over all the data between 0 and 450°C. RK—REDLICH and KWONG (1949), LK—LEE and KESLER (1975), KJ—KERRICK and JACOBS (1981), IUPAC—International Union of Pure and Applied Chemistry, DMW-Eqn. (1) of this study. The symbols are calculated value.

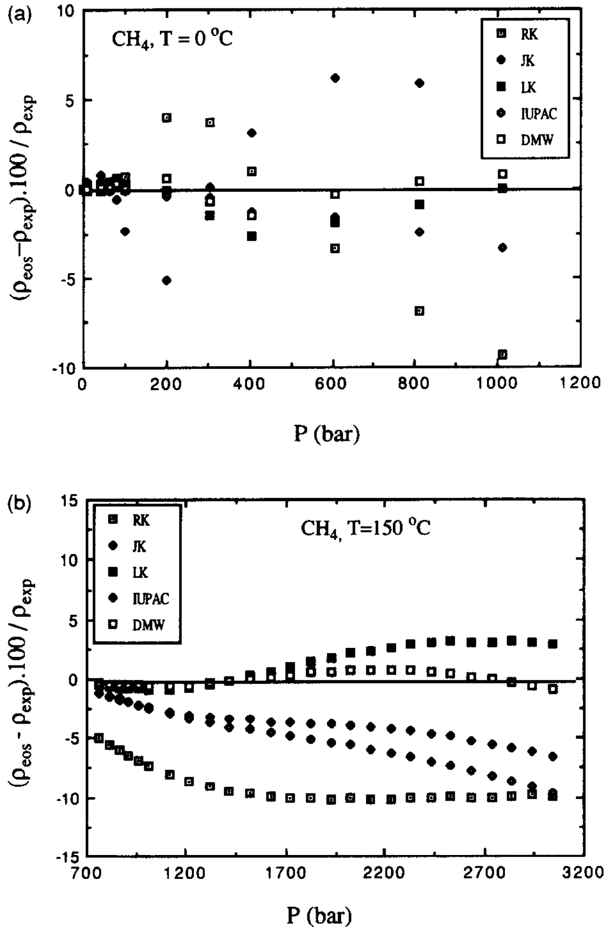

FIG. 3. Comparison of the experimental density of CH_4 with predictions by the EOS of REDLICH-KWONG (RK), JACOBS-KERRICK (JK), LEE-KESLER (LK), International Union of Pure and Applied Chemistry (IUPAC), and Eqn. (1) (DMW). Data of MICHELS and NEDERBRAGT (1936) and DEFFET and FICKS (1965).

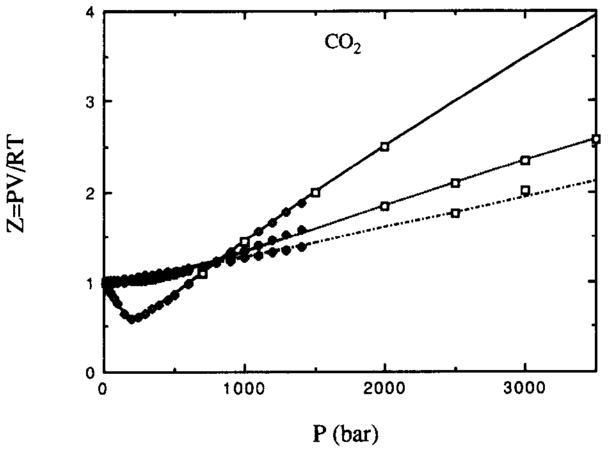

FIG. 4. Comparison of the experimental compressibility factor of CO_2 with predictions of Eqn. (1). Solid line = 100°C; dotted line = 400°C; dot-dash line = 900°C. Symbols: ◆, KENNEDY (1954); ■, VUKALOVICH and ALTUNIN (1968); □, JUZA et al. (1965).

$$C = a_4 + \frac{a_5}{T_r^2} + \frac{a_6}{T_r^3} \tag{2b}$$

$$D = a_7 + \frac{a_8}{T_r^2} + \frac{a_9}{T_r^3} \tag{2c}$$

$$E = a_{10} + \frac{a_{11}}{T_r^2} + \frac{a_{12}}{T_r^3} \tag{2d}$$

$$F = \frac{\alpha}{T_r^3} \tag{2e}$$

$$P_r = \frac{P}{P_c} \tag{3}$$

$$T_r = \frac{T}{T_c} \tag{4}$$

$$V_r = \frac{V}{V_c} \tag{5}$$

where V_c is not the critical volume, but is defined as

$$V_c = \frac{RT_c}{P_c}. \tag{6}$$

The LK and BWR equations were originally used in a corresponding states approach to mixtures. However, in our application all the constants in Eqns. (1)-(5) are assumed to belong to one specific subsystem and are different for each subsystem.

In Eqns. (3)-(4) P_r and T_r are considered to be independent variables. The molar volume V or the inverse density, which is an important quantity in many studies, is a dependent variable derived from the solution to these equations as follows. Given T and P, (a) calculate T_r and P_r using Eqns. (3) and (4), (b) substitute T_r and P_r into Eqn. (1), V_r can be calculated by a variety of methods of solving nonlinear equations; (c) molar volume can be calculated using Eqns. (5) and (6).

In Table 1 we have summarized the data that we have used for the pure systems. All of these data except that which we

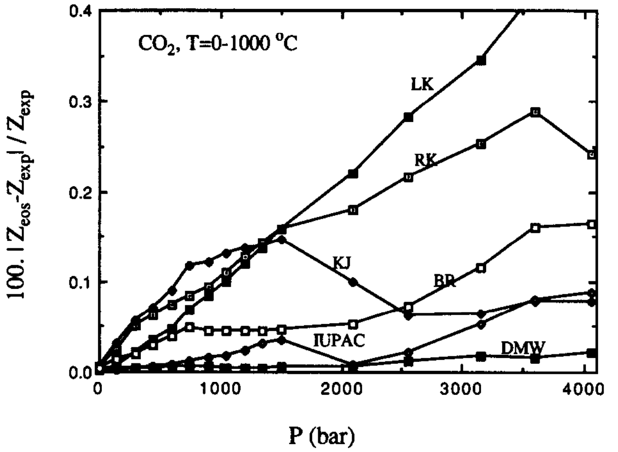

FIG. 5. The deviation of the experimental compressibility factor of CO_2 from predictions of Eqn. (1) and other published EOS. The deviation $\frac{|Z_{cal} - Z_{exp}|}{Z_{exp}}$ is the average value over all the data between 0 and 1000°C. The symbols are calculated values. (RK—REDLICH and KWONG, LK—LEE and KESLER, BR—BOTTINGA and RICHET, KJ—KERRICK and JACOBS, IUPAC—International Union of Pure and Applied Chemistry, DMW—Eqn. (1) of this study).

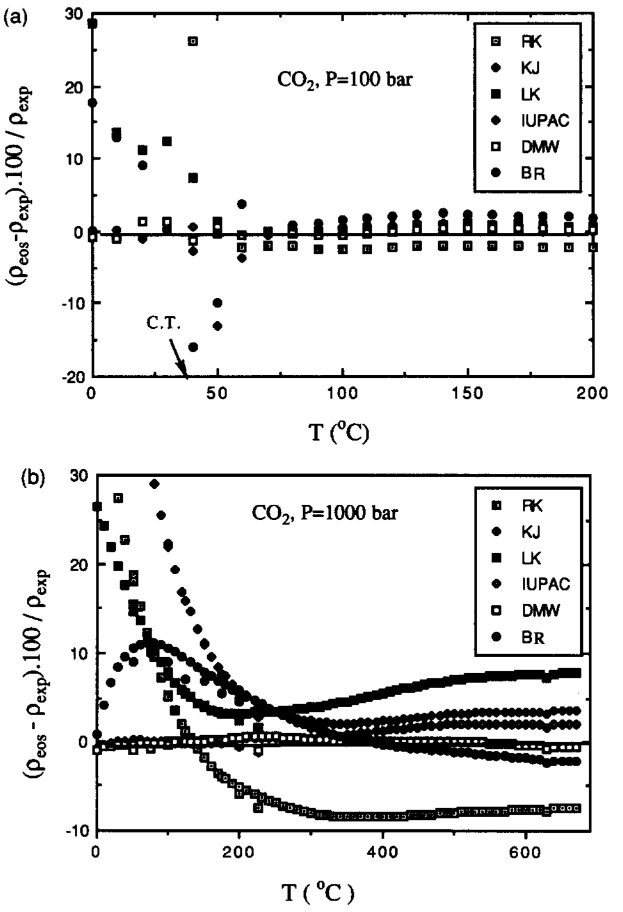

FIG. 6. Comparison of the experimental density of CO_2 (VUKALOVICH et al., 1963; KENNEDY, 1954; and JUZA et al., 1965) with predictions by the EOS of REDLICH and KWONG (RK), JACOBS and KERRICK (JK), LEE and KESLER (LK), BOTTINGA and RICHET (BR), International Union of Pure and Applied Chemistry (IUPAC, ANGUS et al., 1976) EOS, and Eqn. (1) (DMW).

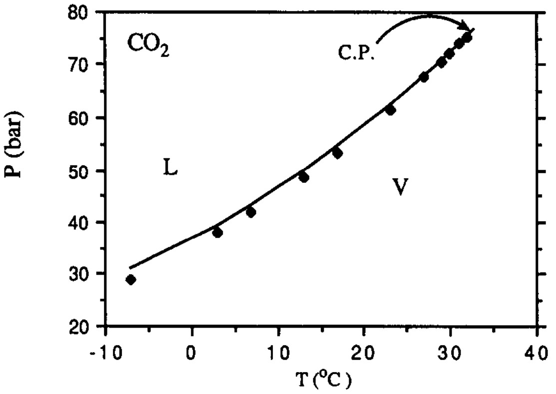

FIG. 7. Comparison of the experimental saturation pressure of CO_2 (ANGUS et al., 1976) with predictions of Eqn. (1). Solid line = Eqn. (1); ◆, ANGUS et al. (1976).

found to be redundant or inconsistent were included in our data base. In individual systems some data outside the range of that used for parameterization were found. Since the distribution of data in the *T-P* space was not uniform for every species, the data above 3500 bar were not included in the parameterization. These measurements were used to evaluate the extrapolation of the EOS.

The large number of data points presented in Table 1 suggests that these pure systems are well described experimentally. The range of the data extends from 0 to 1000°C and from 0 to 8900 bar. However, the coverage is not consistent. For example, in the CH_4 system we have not been able to find data for temperatures above 450°C. This may create a problem for the mixture model in systems of substantial concentration of CH_4 and at high temperature. However, as we will show, the EOS that we have chosen allows the extrapolation in the H_2O well beyond the *T-P* range of the data. If we assume this to be also true for CH_4, the model should be highly accurate for all the pure systems in the range from 0 to 1000°C and 0 to 8000 bar.

The data listed in Table 1 were used to establish the

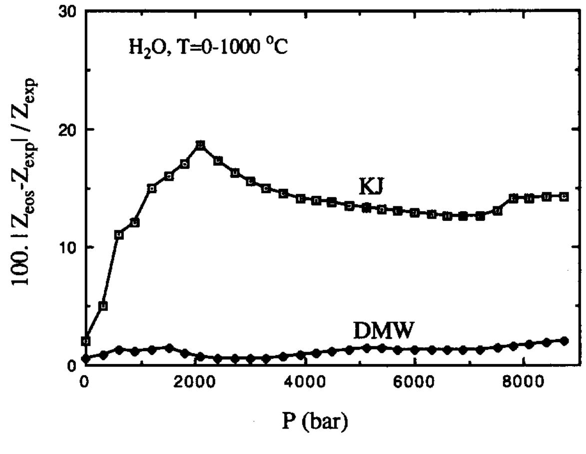

FIG. 8. Comparison experimental compressibility factor of H_2O with predictions of Eqn. (1) and KJ EOS. $\frac{|Z_{cal} - Z_{exp}|}{Z_{exp}}$ is the average value over all the data between 0 and 1000°C. The experimental data are from BURNHAM et al. (1969) and D'ANS et al. (1967).

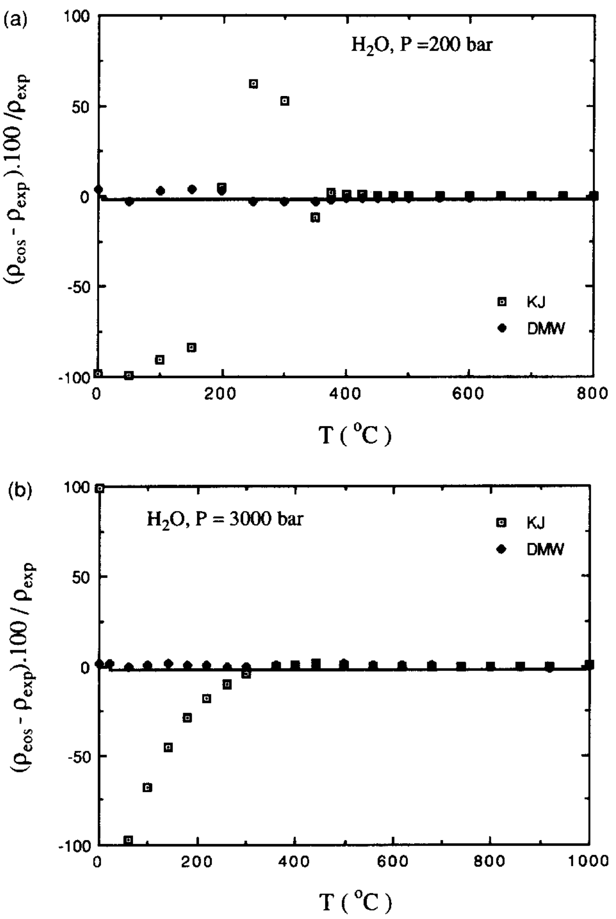

FIG. 9. Comparison of the calculated density of H_2O from Eqn. (1) and KJ EOS with experimental data (D'ANS, 1967; MAIER and FRANK, 1968; BURNHAM et al., 1969).

parameters for all three pure systems. The relations $(\partial P_r/\partial V_r)_{T_r} = 0$, $(\partial^2 P_r/\partial V_r^2)_{T_r} = 0$ are imposed as additional data at the critical point. They improved the quality of predictions in the critical region. Along the liquid-vapor saturation line, both liquid and vapor PVT data were used.

The CH_4 System

Of the three subsystems this is the most ideal. Its critical parameters are given in Table 2. For CH_4 the critical temperature is well below the range of interest in this work. Nevertheless, as illustrated in Fig. 1, the system shows strong nonideal behavior at high pressure. 1083 data points, covering a temperature range 0–450°C and pressure range 0–3500 bar, were used for fitting the EOS with an average error of 0.466%. Except for the small part of the data of FRANCESCONI (1978), all data are consistent within a discrepancy of 0.1–0.5%. The parameters for Eqn. (1) are collected in Table 3.

Other EOS for this system have been published. The four which are thought to be the most reliable are RK EOS, LK EOS, JK EOS, and the equation of MCCARTY (1974). The MCCARTY (1974) equation was recommended by IUPAC (ANGUS et al., 1978). Comparisons of experimental data with the predictions of these equations and Eqn. (1) are shown in Fig. 2. Equation (1) and the IUPAC EOS are the most accurate for pressures below 700 bar and temperatures below 450°C. However, for pressures above 700 bar, Eqn. (1) is the only EOS that produces predictions within experimental accuracy (Fig. 3a,b). The EOS by SAXENA and FEI (1987) and by BELONOSHKO and SAXENA (1991) is applicable at high pressures (>5000 bar). However, in the pressure range of this study, they are far inferior to Eqn. (1).

The CO_2 System

The critical temperature and pressure for this system are given in Table 2. For temperatures within the range of the model, both liquid and gaseous behavior are possible. A plot of the compressibility factor vs. pressure (Fig. 4) shows both positive and negative deviations from ideal behavior at low temperatures. 3360 experimental data points (Table 1), covering a range of 0–1000°C and 0–3500 bar, were used. All the data sets are within an error of about 0.1–0.5%. SHMONOV and SHMULOVICH (1974) reported 48 data points from 408–707°C and from 500–8000 bar. The largest deviation between this data set and others is about 2.5%. This data set is not used in the parameterization. VUKALOVICH and ALTUNIN (1968) questioned the accuracy of the data of KENNEDY (1954). However, our calculations show that the discrepancy between their data and that of others is about 0.3% in specific volume or about the same as experimental uncertainty. Therefore, except for the data of AMAGAT (1892), which are in the same range as the data of MICHELS et al. (1935), all the data of Table 1 were used. The parameters are listed in Table 3.

The predictions of Eqn. (1) are compared to RK EOS, LK EOS, KJ EOS, BOTTINGA and RICHET (1981; hereinafter BR), IUPAC EOS (see ANGUS et al., 1976) in Figs. 5–6. The RK EOS and the LK EOS are reliable below 100 bar for most temperatures in the range 0–1000°C. The BR EOS has average error of 4–5% in the entire T-P range. The KJ EOS is reliable below 200 bar for $T \approx$ 35–350°C and below 450 bar or above 2000 bar for $T \approx$ 350–800°C. The IUPAC EOS is found to be reliable below 1000 bar for $T \approx$ −53–900°C. The IUPAC EOS is superior to Eqn. (1) in the subcritical region below 31°C. However, this EOS is too complicated

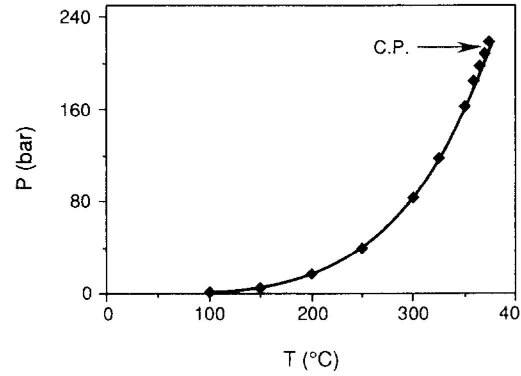

FIG. 10. Comparison of the predicted saturation pressure of H_2O with experimental data (HAAR et al., 1984). Solid line = Eqn. (1); ◆, steam table by HAAR et al. (1984).

Table 4 Fugacity Coefficients of CH_4 Calculated from Eq. (10)

P (bar)	T (°C)									
	0	100	200	300	400	500	600	800	1000	1200
1	0.9977	0.9994	0.9999	1.0001	1.0002	1.0003	1.0003	1.0003	1.0002	1.0002
20	0.9553	0.9873	0.9984	1.0027	1.0044	1.0051	1.0053	1.0051	1.0046	1.0042
50	0.8915	0.9697	0.9967	1.0071	1.0113	1.0129	1.0133	1.0128	1.0117	1.0106
100	0.7968	0.9442	0.9959	1.0158	1.0237	1.0266	1.0272	1.0259	1.0237	1.0215
200	0.6725	0.9099	1.0017	1.0376	1.0516	1.0563	1.0568	1.0534	1.0484	1.0437
300	0.6223	0.8991	1.0179	1.0655	1.0835	1.0266	1.0887	1.0823	1.0743	1.0668
400	0.6124	0.9086	1.0443	1.0994	1.1196	1.1246	1.1229	1.1128	1.1012	1.0907
500	0.6263	0.9345	1.0802	1.1393	1.1597	1.1632	1.1594	1.1448	1.1292	1.1153
600	0.6565	0.9737	1.1249	1.1851	1.2040	1.2050	1.1983	1.1783	1.1582	1.1408
700	0.7000	1.0247	1.1779	1.2366	1.2525	1.2498	1.2397	1.2134	1.1884	1.1671
800	0.7556	1.0865	1.2388	1.2939	1.3051	1.2979	1.2834	1.2501	1.2196	1.1942
900	0.8229	1.1588	1.3076	1.3569	1.3620	1.3491	1.3297	1.2884	1.2520	1.2221
1000	0.9024	1.2417	1.3843	1.4256	1.4232	1.4036	1.3785	1.3283	1.2856	1.2509
1200	1.1014	1.4404	1.5621	1.5810	1.5588	1.5228	1.4841	1.4134	1.3563	1.3111
1400	1.3628	1.6874	1.7746	1.7615	1.7130	1.6560	1.6007	1.5056	1.4319	1.3749
1600	1.7015	1.9900	2.0256	1.9691	1.8871	1.8043	1.7289	1.6053	1.5126	1.4424
1800	2.1374	2.3578	2.3197	2.2066	2.0826	1.9686	1.8694	1.7128	1.5988	1.5138
2000	2.6964	2.8027	2.6630	2.4770	2.3015	2.1500	2.0230	1.8286	1.6905	1.5892
2200	3.4116	3.3391	3.0623	2.7842	2.5458	2.3501	2.1907	1.9530	1.7881	1.6689
2400	4.3252	3.9846	3.5258	3.1324	2.8182	2.5702	2.3734	2.0867	1.8919	1.7529
2600	5.4910	4.7603	4.0629	3.5263	3.1211	2.8120	2.5722	2.2301	2.0022	1.8415
2800	6.9773	5.6912	4.6845	3.9715	3.4579	3.0775	2.7882	2.3838	2.1192	1.9349
3000	8.8705	6.8073	5.4030	4.4741	3.8317	3.3685	3.0229	2.5485	2.2432	2.0331
3200	11.280	8.1444	6.2330	5.0409	4.2463	3.6874	3.2776	2.7247	2.3748	2.1366
3400	14.345	9.7448	7.1910	5.6798	4.7059	4.0366	3.5538	2.9132	2.5142	2.2454
3600	18.241	11.659	8.2958	6.3993	5.2150	4.4186	3.8531	3.1147	2.6618	2.3599
3800	23.189	13.948	9.5692	7.2091	5.7786	4.8364	4.1774	3.3300	2.8180	2.4802
4000	29.469	16.682	11.036	8.1202	6.4022	5.2930	4.5286	3.5601	2.9834	2.6067
4200	37.439	19.946	12.725	9.1444	7.0919	5.7919	4.9086	3.8057	3.1583	2.7395
4400	47.529	23.840	14.668	10.296	7.8542	6.3367	5.3198	4.0678	3.3432	2.8790
4600	60.314	28.484	16.902	11.588	8.6965	6.9314	5.7644	4.3476	3.5388	3.0255
4800	76.495	34.019	19.471	13.040	9.6267	7.5803	6.2451	4.6460	3.7454	3.1793
5000	96.960	40.612	22.422	14.669	10.654	8.2881	6.7646	4.9642	3.9638	3.3407
5500	174.91	63.111	31.854	19.660	13.710	10.349	8.2530	5.8545	4.5648	3.7796
6000	314.24	97.779	45.144	26.295	17.611	12.904	10.055	6.8976	5.2532	4.2740
6500	562.257	151.024	63.818	35.094	22.579	16.062	12.233	8.118	6.041	4.830
7000	1001.891	232.539	89.986	46.736	28.895	19.960	14.862	9.543	6.940	5.455
7500	1778.045	356.953	126.566	62.104	36.909	24.763	18.030	11.207	7.966	6.157
8000	3142.950	546.276	177.574	82.352	47.056	30.672	21.841	13.145	9.137	6.944
8500	5534.102	833.543	248.535	108.974	59.885	37.930	26.420	15.402	10.470	7.827
9000	9707.747	1268.214	347.028	143.908	76.076	46.831	31.915	18.025	11.986	8.815
9500	16966.79	1924.157	483.437	189.664	96.476	57.732	38.499	21.073	13.711	9.921
10000	29584.79	2911.439	671.958	249.488	122.138	71.064	46.379	24.609	15.670	11.158

to use in a mixing model and inferior to Eqn. (1) for pressures above 1000 bar. As in the system CH_4, the EOS by SAXENA and FEI (1987) and by BELONOSHKO and SAXENA (1991) are far from accurate for pressures below 5000 bar. It has reasonable accuracy for pressures above 5000 bar.

With the exception of Eqn. (1) and the IUPAC equation, all the EOS have very poor prediction below and just above the critical temperature. It is difficult to fit the critical region (31 ± 5°C) with a single EOS as noticed by ANGUS et al. (1976). The EOS of this study is not as accurate as the IUPAC EOS in the critical region and subcritical region (below 31°C). In the critical region, the error in density of Eqn. (1) can be 6%. Along the saturation line, the error is about 1-2%. However, it is possible to predict the onset of two-phase behavior. The predicted vapor pressure of CO_2 fluids is given in Fig. 7. For geological applications the two-phase region of this EOS above 0°C is satisfactory.

The H_2O System

The critical parameters for this system are well into the range of this model. A number of important geological applications fall in the liquid region. For example, in shallow geothermal systems the pressures are typically below 700 bar with temperatures below 300°C. There is a great deal of PVT data, from which we choose the data listed in Table 1. (The results of MAIER and FRANK (1968) overlap with other data and were not included.) The data of BURNHAM et al. (1969) is consistent with the data of D'ANS et al. (1967), and have been widely accepted (KERRICK and JACOBS, 1981; FISHER, 1976). No data above 3500 bar were used in our fitting, because it was not possible to fit the liquid phase region if these results were given significant weight. Instead we used the data beyond 3500 bar to test the extrapolation properties of our EOS. Quite reliable results were obtained (see Section IV).

Table 5 Fugacity Coefficients of CO_2 Calculated from Eq. (10)

P (bar)	T(°C)									
	0	100	200	300	400	500	600	800	1000	1200
1	0.9931	0.9976	0.9991	0.9997	1.0000	1.0001	1.0002	1.0002	1.0002	1.0002
20	0.8648	0.9537	0.9825	0.9941	0.9993	1.0018	1.0031	1.0040	1.0041	1.0039
50	0.5695	0.8870	0.9574	0.9857	0.9985	1.0047	1.0078	1.0100	1.0102	1.0098
100	0.3152	0.7839	0.9184	0.9731	0.9980	1.0101	1.0162	1.0204	1.0207	1.0198
200	0.1914	0.6186	0.8530	0.9535	1.0003	1.0232	1.0345	1.0422	1.0424	1.0402
300	0.1538	0.5264	0.8062	0.9420	1.0071	1.0101	1.0550	1.0654	1.0650	1.0615
400	0.1383	0.4817	0.7780	0.9386	1.0186	1.0583	1.0778	1.0900	1.0887	1.0835
500	0.1321	0.4612	0.7656	0.9432	1.0348	1.0807	1.1029	1.1161	1.1134	1.1062
600	0.1310	0.4549	0.7654	0.9553	1.0557	1.1062	1.1305	1.1437	1.1391	1.1298
700	0.1332	0.4578	0.7748	0.9741	1.0811	1.1351	1.1606	1.1728	1.1660	1.1541
800	0.1380	0.4676	0.7919	0.9990	1.1111	1.1673	1.1932	1.2037	1.1939	1.1793
900	0.1449	0.4828	0.8156	1.0294	1.1453	1.2028	1.2283	1.2361	1.2231	1.2053
1000	0.1537	0.5029	0.8451	1.0651	1.1838	1.2416	1.2661	1.2704	1.2534	1.2323
1200	0.1770	0.5560	0.9201	1.1512	1.2729	1.3292	1.3498	1.3442	1.3179	1.2889
1400	0.2085	0.6259	1.0153	1.2564	1.3783	1.4300	1.4443	1.4253	1.3876	1.3493
1600	0.2494	0.7136	1.1312	1.3808	1.5003	1.5447	1.5501	1.5143	1.4628	1.4138
1800	0.3018	0.8210	1.2691	1.5256	1.6395	1.6736	1.6677	1.6113	1.5437	1.4825
2000	0.3683	0.9511	1.4312	1.6922	1.7972	1.8177	1.7977	1.7167	1.6306	1.5556
2200	0.4525	1.1076	1.6206	1.8828	1.9746	1.9779	1.9408	1.8311	1.7238	1.6332
2400	0.5587	1.2951	1.8406	2.0997	2.1737	2.1554	2.0979	1.9548	1.8235	1.7157
2600	0.6926	1.5192	2.0956	2.3460	2.3962	2.3517	2.2700	2.0885	1.9301	1.8032
2800	0.8615	1.7865	2.3904	2.6249	2.6446	2.5683	2.4581	2.2326	2.0439	1.8958
3000	1.0743	2.1051	2.7308	2.9404	2.9214	2.8069	2.6636	2.3878	2.1653	1.9939
3200	1.3427	2.4847	3.1235	3.2968	3.2294	3.0694	2.8876	2.5548	2.2947	2.0977
3400	1.6810	2.9366	3.5760	3.6990	3.5719	3.3580	3.1316	2.7343	2.4324	2.2074
3600	2.1077	3.4744	4.0973	4.1525	3.9523	3.6750	3.3973	2.9272	2.5790	2.3232
3800	2.6458	4.1143	4.6973	4.6636	4.3746	4.0230	3.6864	3.1343	2.7349	2.4456
4000	3.3245	4.8754	5.3878	5.2393	4.8431	4.4047	4.0007	3.3565	2.9007	2.5748
4200	4.1807	5.7805	6.1820	5.8874	5.3627	4.8232	4.3422	3.5948	3.0768	2.7111
4400	5.2609	6.8567	7.0951	6.6167	5.9386	5.2819	4.7132	3.8503	3.2638	2.8549
4600	6.6237	8.1361	8.1448	7.4372	6.5768	5.7843	5.1161	4.1241	3.4624	3.0064
4800	8.3431	9.6567	9.3509	8.3598	7.2835	6.3346	5.5533	4.4174	3.6731	3.1662
5000	10.512	11.464	10.7366	9.3969	8.0661	6.9369	6.0277	4.7315	3.8967	3.3345
5500	18.753	17.611	15.168	12.586	10.4072	8.7027	7.3967	5.6170	4.5169	3.7956
6000	33.476	27.059	21.422	16.847	13.419	10.9107	9.0710	6.6654	5.2344	4.3200
6500	59.764	41.561	30.233	22.532	17.286	13.667	11.116	7.905	6.063	4.916
7000	106.650	63.791	42.631	30.105	22.245	17.103	13.609	9.368	7.020	5.592
7500	190.180	97.823	60.047	40.175	28.593	21.378	16.644	11.094	8.123	6.358
8000	338.799	149.846	84.477	53.547	36.708	26.693	20.336	13.127	9.394	7.226
8500	602.863	229.258	118.695	71.279	47.067	33.289	24.820	15.518	10.856	8.208
9000	1071.365	350.305	166.553	94.756	60.272	41.466	30.259	18.330	12.537	9.318
9500	1901.339	534.546	233.394	125.798	77.084	51.590	36.850	21.631	14.467	10.572
10000	3369.441	814.565	326.616	166.788	98.460	64.109	44.828	25.504	16.683	11.989

The KJ EOS are compared to Eqn. (1) and the experimental data in Figs. 8, 9a, and b. Because of the strong polarity of H_2O, the LK EOS and RL EOS are only reliable (within 1%) below 20 bar over the temperature range considered. By adding 3 polar parameters to the Benedict-Webb-Rubin-Starling equation, NISHIUMI (1980b) developed an EOS reliable from 200–800°C for pressures below 300 bar. The KJ EOS is reliable only for temperature above the critical point of H_2O (see Fig. 9a,b).

There is considerable application for models of the two-phase coexistence or gas solubility in this system. Just as in the CO_2 system, our results show that this model can describe the liquid-vapor equilibrium with accuracies close to that of experimental measurements. In two-phase and critical region, its predictions are not as accurate as the NBS/NRC steam tables (HAAR et al., 1984). In the critical region, the largest error in density is about 3%, and along the saturation line the error in density is about 1%. As shown in Fig. 10 the vapor pressure of pure water is quite accurately predicted. For supercritical temperatures Eqn. (1) is as accurate as the equation suggested by the NBS/NRC (HAAR et al., 1984).

III. CALCULATION OF FUGACITY COEFFICIENTS

A primary objective of this work is the calculation of fugacities or free energies. These will be used in future calculations of phase equilibria. The fugacity is defined by

$$\mu(T) = \mu^0(T) + RT \ln f(T, P). \tag{7}$$

The fugacity coefficient

$$\phi(T, P) = \frac{f}{P} \tag{8}$$

is usually reported. It may be calculated from Eqns. (1)–(8) using the relation (WALAS, 1985)

Table 6 Fugacity Coefficients of H_2O Calculated from Eq. (10)

P (bar)	T (°C)									
	0	100	200	300	400	500	600	800	1000	1200
1	0.1831	0.9890	0.9950	0.9974	0.9986	0.9991	0.9995	0.9998	0.9999	1.0000
20	0.0095	0.0875	0.7615	0.9491	0.9713	0.9830	0.9897	0.9962	0.9989	1.0002
50	0.0033	0.0356	0.3095	0.8737	0.9290	0.9579	0.9743	0.9905	0.9973	1.0005
100	0.0017	0.0184	0.1589	0.6628	0.8598	0.9168	0.9492	0.9812	0.9947	1.0011
200	0.0009	0.0098	0.0837	0.3490	0.7244	0.8378	0.9008	0.9631	0.9898	1.0023
300	0.0007	0.0069	0.0588	0.2448	0.5808	0.9168	0.8549	0.9460	0.9851	1.0036
400	0.0005	0.0055	0.0464	0.1930	0.4672	0.6935	0.8118	0.9297	0.9808	1.0051
500	0.0005	0.0047	0.0391	0.1621	0.3962	0.6311	0.7719	0.9143	0.9769	1.0067
600	0.0004	0.0041	0.0343	0.1418	0.3486	0.5781	0.7353	0.8998	0.9732	1.0085
700	0.0004	0.0038	0.0309	0.1275	0.3146	0.5349	0.7025	0.8863	0.9699	1.0105
800	0.0004	0.0035	0.0284	0.1169	0.2892	0.5000	0.6734	0.8738	0.9670	1.0125
900	0.0004	0.0033	0.0266	0.1089	0.2698	0.4717	0.6480	0.8623	0.9644	1.0148
1000	0.0003	0.0031	0.0251	0.1026	0.2545	0.4487	0.6258	0.8517	0.9622	1.0172
1200	0.0003	0.0029	0.0231	0.0937	0.2324	0.4141	0.5902	0.8334	0.9589	1.0225
1400	0.0003	0.0028	0.0219	0.0878	0.2175	0.3901	0.5637	0.8188	0.9569	1.0284
1600	0.0003	0.0028	0.0211	0.0839	0.2074	0.3732	0.5442	0.8075	0.9564	1.0350
1800	0.0003	0.0027	0.0206	0.0814	0.2005	0.3614	0.5302	0.7993	0.9574	1.0424
2000	0.0004	0.0028	0.0204	0.0799	0.1959	0.3533	0.5203	0.7939	0.9596	1.0504
2200	0.0004	0.0028	0.0204	0.0790	0.1931	0.3480	0.5138	0.7909	0.9633	1.0592
2400	0.0004	0.0029	0.0205	0.0788	0.1916	0.3449	0.5100	0.7902	0.9682	1.0687
2600	0.0004	0.0030	0.0208	0.0791	0.1913	0.3437	0.5084	0.7914	0.9744	1.0790
2800	0.0005	0.0031	0.0212	0.0797	0.1919	0.3440	0.5087	0.7944	0.9818	1.0900
3000	0.0005	0.0032	0.0217	0.0808	0.1933	0.3455	0.5107	0.7991	0.9904	1.1018
3200	0.0005	0.0034	0.0223	0.0821	0.1954	0.3483	0.5142	0.8052	1.0000	1.1144
3400	0.0006	0.0035	0.0230	0.0838	0.1981	0.3520	0.5190	0.8128	1.0108	1.1277
3600	0.0006	0.0037	0.0237	0.0857	0.2014	0.3566	0.5249	0.8216	1.0226	1.1417
3800	0.0007	0.0039	0.0246	0.0879	0.2053	0.3621	0.5319	0.8317	1.0354	1.1566
4000	0.0008	0.0041	0.0255	0.0904	0.2096	0.3684	0.5400	0.8428	1.0492	1.1721
4200	0.0008	0.0044	0.0266	0.0931	0.2145	0.3754	0.5490	0.8551	1.0639	1.1884
4400	0.0009	0.0047	0.0277	0.0960	0.2198	0.3832	0.5589	0.8684	1.0796	1.2055
4600	0.0010	0.0050	0.0290	0.0992	0.2256	0.3916	0.5697	0.8828	1.0961	1.2233
4800	0.0011	0.0053	0.0303	0.1027	0.2319	0.4008	0.5813	0.8981	1.1136	1.2418
5000	0.0012	0.0056	0.0317	0.1064	0.2387	0.4106	0.5938	0.9144	1.1320	1.2611
5500	0.0016	0.0066	0.0358	0.1168	0.2576	0.4380	0.6286	0.9592	1.1817	1.3124
6000	0.0020	0.0079	0.0407	0.1290	0.2795	0.4697	0.6685	1.0098	1.2369	1.3684
6500	0.0026	0.0094	0.0464	0.1432	0.3046	0.5057	0.7136	1.0662	1.2974	1.4290
7000	0.0034	0.0113	0.0531	0.1595	0.3333	0.5463	0.7641	1.1286	1.3635	1.4943
7500	0.0044	0.0135	0.0610	0.1783	0.3656	0.5919	0.8203	1.1969	1.4351	1.5645
8000	0.0057	0.0163	0.0703	0.1997	0.4022	0.6427	0.8824	1.2716	1.5125	1.6396
8500	0.0074	0.0197	0.0812	0.2243	0.4433	0.6992	0.9509	1.3528	1.5959	1.7199
9000	0.0097	0.0238	0.0939	0.2523	0.4894	0.7619	1.0262	1.4410	1.6855	1.8054
9500	0.0126	0.0288	0.1088	0.2842	0.5411	0.8313	1.1089	1.5366	1.7817	1.8964
10000	0.0165	0.0350	0.1262	0.3206	0.5991	0.9081	1.1995	1.6399	1.8846	1.9932

$$\ln \phi(T,P) = \int_0^P (Z-1)\frac{dP}{P}$$

$$= Z - 1 - \ln Z - \int_\infty^{V_r}\left(\frac{P_r}{T_r} - \frac{1}{V_r}\right)dV_r. \quad (9)$$

Using Eqn (1), Eqn. (9) gives

$$\ln \phi(T,P) = Z - 1 - \ln Z + \frac{B}{V_r}$$

$$+ \frac{C}{2V_r^2} + \frac{D}{4V_r^4} + \frac{E}{5V_r^5} + G, \quad (10)$$

where

$$G = \frac{F}{2\gamma}\left[\beta + 1 - \left(\beta + 1 + \frac{\gamma}{V_r^2}\right)\exp\left(-\frac{\gamma}{V_r^2}\right)\right], \quad (11)$$

Table 7 Comparison of Eq.(1) with Data Beyond Fitting Region Molar Volume of CH_4

T (°C)	P (bar)	Eq.(1)	data by Vennix et al. (1970)
-49.32	38.48	398.0	392.
-33.35	42.59	395.25	392.
-20.32	45.90	393.89	392.
-10.28	48.56	393.41	392.
-29.38	88.94	158.39	155.
-10.96	103.61	156.10	155.
-43.1	83.61	146.29	155.
-24.71	100.76	141.37	138.7
-20.30	105.76	140.69	138.6
-10.11	114.23	139.78	138.6
-48.13	225.97	55.66	57.
-40.07	259.96	55.97	57.
-14.51	366.60	56.57	57.
-6.4	400.09	56.69	57.

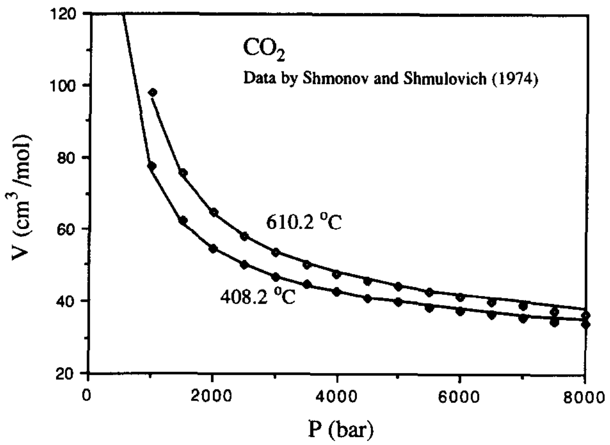

FIG. 11. Comparison experimental molar volume of CO_2 with predictions of Eqn. (1).

with V_r calculated as in the last section. Equation (10) may be used to calculate the fugacity and the free energy for a given T and P. We have compiled fugacity coefficients for CH_4, CO_2, and H_2O for a number of temperature and pressure conditions (Tables 4–6). Nonideality can be quite large for temperatures and pressure typical of geological environments.

IV. DISCUSSION

Before we proceed with applications of this EOS, we discuss the accuracy of the predictions for intensive variable values beyond the range of data used in the parameterization. This range was chosen with the objective of having a fairly uniform distribution of data over the three subsystems. As we mentioned earlier, this is not possible because of the limitation of CH_4 data to the relatively low temperature range (see Table 1). It is expected that a system will behave more ideally as the temperature is raised and the pressure is lowered. This suggests that the extrapolation to higher temperature will not decrease the accuracy substantially. An idea of the extrapolation to more nonideal conditions can be obtained by observing the quality of the predictions at high pressure. Some results of the application of the CH_4 EOS have been included in Fig. 1. The accuracy is maintained up to 8000 bar, whereas the parameterization only included data to 3500 bar. Comparison of this EOS with experimental data below 0°C indicates that it is reliable (within 3%) even below −40°C to about 100 bar (see Table 7). For the CO_2 system, the data set of SHMONOV and SHMULOVICH (1974) is the only one which covers pressures up to 8000 bar. Comparison of this data set with Eqn. (1) indicates that the discrepancy is about 2.5% (Fig. 11). This is also the discrepancy between this data set and others.

Table 8 Comparison of eq.(1) with Data Beyond Fitting Region
Molar volume of H_2O

T (°C)	P (bar)	Eq.(1)	NBS/NRC steam table
1200	100	1226.2	1224.3
1600	100	1566.4	1564.0
2000	100	1902.8	1900.3
1200	1000	125.5	124.2
1600	1000	164.8	163.3
2000	1000	201.3	199.7
1200	5000	34.0	33.58
1600	5000	42.1	41.49
2000	5000	50	49.18
1200	10000	24.5	23.47
1600	10000	28.4	27.15
2000	10000	32.2	30.82

Another test of the general ability of our form to accurately predict very high temperature and pressure data is given by the H_2O EOS. Data for this system extend over a large range of pressures and temperatures. In Fig. 12 we compare the model to extensive data of BURNHAM et al. (1969), which is outside the range of parameterization. Further support for the model may be obtained from the NBS/NRC Steam Table. The model is within 4.5% of those given in the table up to 2000°C and 10,000 bar (see Table 8).

We have demonstrated that there are large deviations from

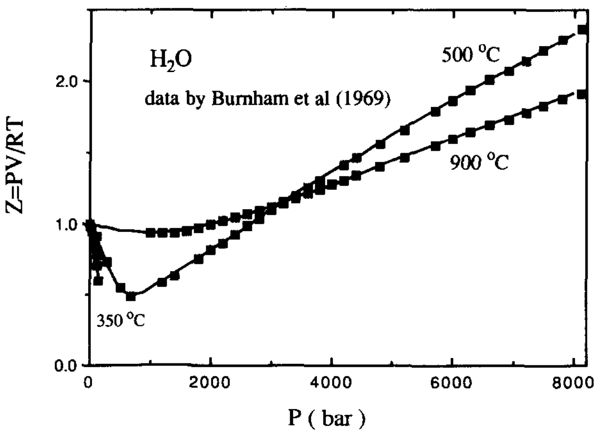

FIG. 12. Comparison of the experimental compressibility factor of H_2O (BURNHAM et al., 1969) with predictions of Eqn. (1) The data above 3500 bar was not used in the parameterization.

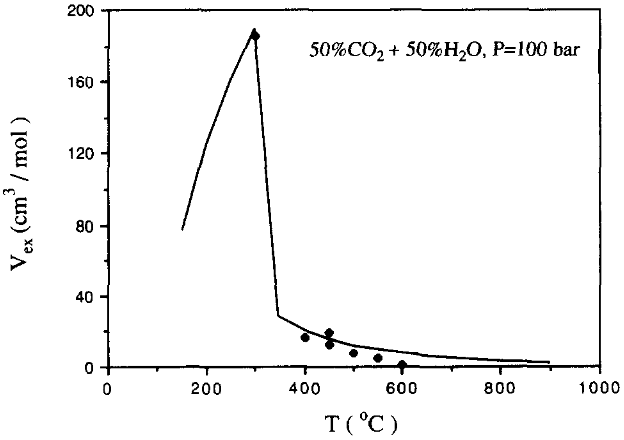

FIG. 13. The molar excess volume of the mixture 50% CO_2 + 50% H_2O at 100 bar and different temperatures. Experimental data from ZAKIROV (1984) and GEHRIG (1980).

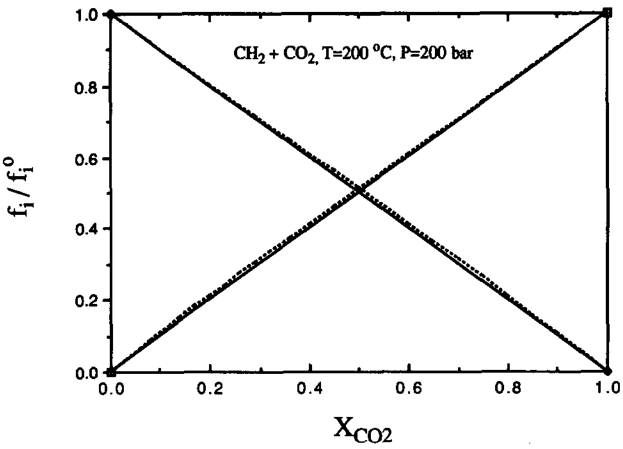

FIG. 14. The activity of CH_4 and CO_2 in their mixtures. The dashed line is ideal mixing activity, and the solid line represents the real activity calculated using the EOS for mixtures described in the following article.

ideal behavior in the endmember systems and that the EOS of this study is able to accurately represent this behavior. In the following article we discuss the generalization of this approach to mixed systems. However, before we develop such a model it is worthwhile to investigate how well an ideal mixing approach will predict the data. We can get an idea of the magnitude of the excess free energy by looking at the excess volumes:

$$V_{ex}^{M} = V^{M} - \sum x_i V_i. \qquad (12)$$

The excess free energy of mixing is directly calculated from an integral of the excess volume over pressure. It follows that if the excess volume is very small for all pressures the excess free energy will be small. In order to illustrate the effect of nonideal mixing, we calculated the excess volume of the system 50% CO_2 + 50% H_2O at 100 bar and varying temperatures (see Fig. 13). The mixing model of the following article was used. It can be seen from Fig. 13 that the excess volume decreases rapidly above 370°C. This implies that mixing is close to ideal at high temperatures. This is true in spite of the fact that the endmember systems may be very nonideal at these temperatures (see Tables 4–6). If the excess volume of mixing is small, a very simple equation for the free energy of mixing, Amagat's rule, holds (PITZER and BREWER, 1961):

$$\phi_i^{M} = x_i \phi_i^{P}, \qquad (13)$$

where ϕ_i^M and ϕ_i^P are the fugacity coefficients of species i in mixture and the pure system, respectively, and x_i is the mole fraction of species in the mixture. ϕ_i^P may be obtained, for example, from tables, from our endmember EOS or directly from data, obviating the use of an EOS for the mixed system. An example for the system CH_4 + CO_2 at 200°C and 200 bar is shown on Fig. 14. In this figure ideal mixing works well. However, in some other cases (for example, the CO_2-H_2O system for temperatures below 350°C), assuming ideal mixing is very inaccurate, as shown in Fig. 13.

Acknowledgments—We thank Drs. J. Dubessy, I. M. Chou, T. Bowers, and an anonymous reviewer for their comments and suggestions for improving the manuscripts. This work has been supported by funds from the Department of Energy: DOE-DE-AC03-88SF, the American Chemical Society, ACS PRF 18991 AC2, and Central Canada Potash. Thanks also to Dr. J. Greenberg for discussions.

Editorial handling: T. Bowers

REFERENCES

AMAGAT E. H. (1892) On the determination of the density of the liquified gas and saturated vapor of the critical point of carbon dioxide. *C. R. Acad. Sci. Paris* **114,** 1093–1098.

ANGUS S., ARMSTRONG B., and REUCK K. M. (1976) International thermodynamic tables of the fluid state-3 Carbon Dioxide. *International Union of Pure and Applied Chemistry, Chemical Data Series 16.*

ANGUS S., ARMSTRONG B., and REUCK K. M. (1978) International thermodynamic tables of the fluid state-5 methane. *International Union of Pure and Applied Chemistry, Chemical Data Series 16.*

BEATTIE J. A. and BRIDGEMAN O. C. (1928) A new equation of state for fluids: II. Application to helium, neon, argon, hydrogen, nitrogen, oxygen, air, and methane. *J. Amer. Chem. Soc.* **50,** 3131–3138.

BELONOSHKO A. and SAXENA S. K. (1991) A molecular dynamics study of the pressure-volume-temperature properties of supercritical fluids: II. CO_2, CH_4, CO, O_2, and H_2. *Geochim. Cosmochim. Acta* **55,** 3191–3280.

BENDER E. (1970) Equations of state exactly representing the phase behavior for pure substance. *Proc. 5th Symposium on thermodynamical properties, American Society of Mechanical Engineers, New York,* 227–235.

BENEDICT M., WEBB G. B., and RUBIN L. C. (1940) An empirical equation for thermodynamic properties of light hydrocarbons and their mixtures. *J. Chem. Phys.* **8,** 334–345.

BOTTINGA Y. and RICHET P. (1981) High pressure and temperature equation of state and calculation of the thermodynamic properties of gaseous carbon dioxide. *Amer. J. Sci.* **281,** 620–659.

BOWERS T. S. and HELGESON H. C. (1983) Calculation of the thermodynamic and geochemical consequences in the system H_2O-CO_2-NaCl on phase relations: Equation of state for H_2O-CO_2-NaCl fluids at high pressures and temperatures. *Geochim. Cosmochim. Acta* **47,** 1247–1275.

BURNHAM C. W., HOLLOWAY J. R., and DAVIS N. F. (1969) The specific volume of water in the range 1000 to 8900 bars, 20 to 900°C. *Amer. J. Sci.* **267-A,** 70–95.

CAPUANO R. M. (1990) Hydrochemical constraints on fluid-mineral equilibria during compaction diagenesis of kerogen-rich geopressured sediments. *Geochim. Cosmochim. Acta* **54,** 1283–1299.

CARROLL J. J. and MATHER A. E. (1989) The solubility of hydrogen sulphide in water from 0 to 90°C. *Geochim. Cosmochim. Acta* **53,** 1163–1170.

CHOU I. M. and WILLIAMS R. J. (1977) Activity of H_2O in CO_2-H_2O at 600°C and pressure to 8 kb (abs.). *GSA. Ann. Mtg.* **9,** 928.

D'ANS J., BARTELS J., BRUGGENCATE P. T., SCHMIDT A., JOOS G., and ROTE W. A. (1967) Thermodynamiche Eigenschaften von Wasser und Wasserdapf (International Skeleton Table). *Landolt-Bornstein* **4-4a,** 534–535.

DEFFET L. and FICKS F. (1965) Advanced thermodynamical properties. *Symposium on Thermodynamical Properties, Purdue University, Lafayette, Indiana,* 107.

DIN F. (1961) *Thermodynamic Functions of Gases.* Butterworths.

DOUSLIN D. R., HARRISON R. H., MOORE R. T., and MCCULLOUGH J. P. (1964) *P-V-T* relations of methane. *J. Chem. Eng. Data* **9,** 358–363.

DUAN Z., MØLLER N., and WEARE J. (1992) The prediction of methane solubility in natural waters to high ionic strength from 0 to 250°C and from 0 to 1600 bar. *Geochim. Cosmochim. Acta* **56,** 1451–1460.

FISHER J. R. (1976) The volumetric properties of H_2O—A graphical portrayal. *J. Res. USGS* **4,** 189–193.

FRANCESCONI A. Z. (1978) Kristische Kurve, Phasengleichgewichte und PVT-daten im system methanol-methan bis 3 kbar und 240°C. Ph.D. Thesis, Univ. Fridericiana Karlsruhe, Germany.

Gehrig M. (1980) Phasengleichgewichte und PVT-daten ternarer mischungen aus wasser, kohlendioxide und Natriumchlorid bis 3 kbar und 550°C. Doctorate dissertation, Univ. Karlsruhe.

Greenwood H. G. (1969) The compressibility of gaseous mixtures of carbon dioxide and water between 0 and 500 bars pressure and 450 and 800°C. *Amer. J. Sci.* **267A,** 191–208.

Haar L., Gallagher J. S., and Kell G. S. (1984) *Steam Tables, Thermodynamic and Transport Properties and Computer Programs for Vapor and Liquid States of Water in SI Unites.* Hemisphere Publishing Co.

Hendel E. M. and Hollister L. S. (1981) An empirical solvus for CO_2H_2O-2.6 wt% salt. *Geochim. Cosmochim. Acta* **45,** 225–228.

Jacobs G. K. and Kerrick D. M. (1981a) Methane: An equation of state with application to the ternary system H_2O-CO_2-CH_4. *Geochim. Cosmochim. Acta* **45,** 607–614.

Jacobs G. K. and Kerrick D. M. (1981b) Devolatilization equilibria in H_2O-CO_2 and H_2O-CO_2-NaCl fluids: An experimental and thermodynamic evaluation at elevated pressures and temperatures. *Amer. Mineral.* **66,** 1135–1153.

Juza J., Kmonicek V., and Sifner O. (1965) Measurements of the specific volume of carbon dioxide in the range of 700–4000 bar and 50–475°C. *Physica* **31,** 1735–1744.

Kennedy G. C. (1954) Pressure-volume-temperature relations in CO_2 at elevated temperatures and pressures. *Amer. J. Sci.* **252,** 225–241.

Van Den Kerkhof A. M. (1990) Isochoric phase diagrams in the systems CO_2-CH_4 and CO_2-N_2: Application to fluid inclusions. *Geochim. Cosmochim. Acta* **54,** 621–629.

Kerrick D. M. and Jacobs G. K. (1981) A modified Redlich-Kwong Equation for H_2O-CO_2 mixtures at elevated pressures and temperatures. *Amer. J. Sci.* **281,** 735–767.

Keyes F. G. and Burks H. G. (1922) The isometrics of gaseous methane. *J. Math. Phys.* **1,** 1403–1409.

Kirillin V. A., Ulybin S. A., and Zherdev E. P. (1969) CO_2 density on 35, 30, 20, and 10°C isotherms at pressures up to 500 bar. *Therm. Eng.* **16,** 137–139.

Kvalnes H. M. and Gaddy V. L. (1931) The compressibility isotherms of methane at pressures to 1000 atms and temperatures from −70 to 200°C. *J. Amer. Chem. Soc.* **53,** 394.

Lee B. I. and Kesler M. G. (1975) A generalized thermodynamic correlation based on three-parameter corresponding states. *AIChE J.* **21,** 510–527.

Lira R. and Ripley E. M. (1990) Fluid inclusion studies of the Rodeo de Los Molles REE and Th deposit, Las Chacras Batholith, Central Argetina. *Geochim. Cosmochim. Acta* **54,** 663–671.

McCormack K. E. and Schneider W. G. (1950) Thermodynamic properties of carbon dioxide at temperatures from 0–600°C, and pressures up to 50 atmospheres. *J. Chem. Phys.* **18,** 1273–1275.

Maier S. and Frank E. U. (1968) The density of water from 200–850°C and from 1000–6000 bar. *Ber. Buns. Physik. Chem.* **70,** 639.

McCarty R. D. (1974) A modified Benedict-Webb-Rubin equation of state for methane using recent experimental data. *Cryogenics* **14,** 276–280.

Michels A. and Michels C. (1935) Isotherms of CO_2 between 0° and 150° and pressures from 16 to 250 atm (amagat densities 16–206). *Proc. Roy. Soc.* **A153,** 201–214.

Michels A. and Nederbragt G. W. (1936) Isotherms of methane between 0 and 150° for densities up to 225 Amagat. Calculated specific heat, energy and entropy in the same region. *Physica* **3,** 569–577.

Michels A., Michels C., and Wouters H. (1935) Isotherms of CO_2 between 70 and 3000 atmospheres (amagat densities between 200 and 600). *Proc. Roy. Soc.* **A153,** 214–224.

Michels A., Blaisse B., and Michels C. (1937) The isotherms of CO_2 in the neighbourhood of the critical point and round coexistence line. *Proc. Roy. Soc.* **A160,** 358–375.

Nishiumi H. (1980a) Thermodynamic property prediction of C_{10} to C_{20} paraffins and their mixtures by the generalized BWR equation of state. *J. Chem. Eng. Japan* **13,** 74–76.

Nishiumi H. (1980b) An improved generalized BWR equation of state with three polar parameters applicable to polar substances. *J. Chem. Eng. Japan* **13,** 178–183.

Olds R. H., Reamer H. H., Sage B. H., and Lacey W. N. (1943) Phase equilibrium in hydrocarbon systems: Volumetric behavior of methane. *Ind. Eng. Chem.* **35,** 922–924.

Pitzer K. S. and Brewer L. (1961) *Thermodynamics.* McGraw-Hill Book Co.

Ramboz C., Schnapper D., and Dubessy J. (1985) The P-$\bar{V}$-T-X-fO_2 evolution of H_2O-CO_2 CH_4-bearing fluid in a wolframite vein: Reconstruction from fluid inclusion studies. *Geochim. Cosmochim. Acta* **49,** 205–219.

Reamer H. H., Olds R. H., Sage B. H., and Lacey W. N. (1944) Phase equilibria in hydrocarbon systems: Methane-carbon dioxide system in the gaseous region. *Ind. Eng. Chem.* **36,** 88–90.

Redlich O. and Kwong J. N. S. (1949) On the thermodynamics of solutions. V. An equation of state. Fugacities of gaseous solutions. *Chem. Rev.* **44,** 233–244.

Robertson S. L. and Babb S. E. (1969) PVT properties of methane and propene to 10kbar and 200°. *J. Chem. Phys.* **51,** 1357–1361.

Roedder E. (1972) The composition of fluid inclusion. Data of Geochemistry (ed. M. Fleisher), *USGS Prof. Paper* **440 JJ,** 164.

Rumble D., Ferry J. M., Hoering T. C., and Boucot A. J. (1982) Fluid flow during metamorphism at the Beaver Brook fossile locality, New Hampshire. *Amer. J. Sci.* **282,** 886–919.

Sass A., Dodge B. F., and Bretton R. H. (1967) Compressibility of gas mixtures: Carbon dioxide-Ethylene system. *J. Chem. Eng. Data* **12,** 168–176.

Saxena S. K. and Fei Y. (1987) High pressure and high temperature fluid fugacities. *Geochim. Cosmochim. Acta* **51,** 783–791.

Schamp H. W., Mason E. A., Richardson A. C. B., and Altman A. (1958) Compressibility and intermolecular forces in gases: Methane. *Physics Fluid* **1,** 329–337.

Schmidt G. W. (1973) Interstitial water composition and geochemistry of deep Gulf Coast shales and sandstones. *AAPG Bull.* **57,** 321–337.

Schmidt V. and McDonald D. A. (1979) The role of secondary porosity in diagenesis. In *Aspects of Diagenesis* (ed. P. A. Scholle and P. R. Schluger); *Soc. Econ. Paleontol. Mineral. Spec. Publ.* **26,** 185–207.

Shmonov V. M. and Shmulovich K. I. (1974) Molal volumes and equations of state of CO_2 at temperatures from 100 to 1000°C and pressures from 2000 to 10,000 bar. *Dolk. Akad. Nauk SSSR* **217,** 205–209 (in Russian).

Tsiklis D. S. and Linshits L. R. (1967) Molar volumes and thermodynamic properties of methane at high pressures and temperatures. *Dokl. Akad. Nauk SSSR* **176,** 423–425.

van der Waals J. H. (1873) On the continuity of the gases and liquid state. Dissertation, Leiden.

Vennix A. J., Leland T. W., and Kobayashi R. (1970) Low-temperature volumetric properties of methane. *J. Chem. Eng. Data* **15,** 238–243.

Vrolijk P. (1987) Tectonically driven fluid flow in the Kodiak accretionary complex, Alaska. *Geology* **15,** 466–469.

Vukalovich M. P. and Altunin V. V. (1968). *Thermodynamical Properties of Carbon Dioxide.* Collet's (in Russian).

Vukalovich M. P., Altunin V. V., and Timoshenko N. I. (1963) Experimental determination of the specific volume of carbon dioxide at temperatures from 40–150°C and pressures up to 600 kg/cm^2. *Teploenerg.* **10,** 85–88 (in Russian).

Vukalovich M. P., Kobelev V. P., and Timoshenko N. I. (1968) Experimental investigation of CO_2 density at temperatures from 0 to 35°C and pressures up to 300 bar. *Therm. Eng.* **15,** 103–106.

Walas M. (1985) *Phase Equilibria in Chemical Engineering.* Butterworth.

Weare J. H. (1987) Models of mineral solubility in concentrated brines with application to field observations. *Rev. Mineral.* **17,** 143.

Zakirov I. V. (1984) The P-V-T relations in the H_2O-CO_2 system at 300 and 400°C. *Geochem. Intl.* **21,1** 13–20.

APPENDIX 1: A BRIEF SURVEY OF EQUATIONS OF STATE

In order to summarize experimental measurements of PVT properties it is beneficial to introduce phenomenological equations of state (EOS). The form of these expressions is chosen to describe the PVT behavior of real gases and contains parameters which are fit to the measured PVT data. With the analytical form, it is usually a simple matter to obtain other thermodynamic functions from the EOS (e.g., by integration of the free energy). There are many phenomenological PVT equations, each of which has some justification in terms of rigorous statistical theories. However, as is the case for most applications to real systems, the theoretical derivations require extreme approximations. The important justification of the derived EOS comes from the quality of the fit of the equation to measured data and the accuracy of interpolations or extrapolations to regions of intensive variables not covered by data sets.

While there are many different forms of EOS equations, they can be broadly classified into those based on the virial EOS, those based on the cubic equation, the BWR type equation, the corresponding state equation, and the perturbed-hard-sphere equation (Walas, 1985). The virial equation has a sound theoretical basis and is correct for all gases at sufficiently high temperature and low pressure. The expansion coefficients in the power series are rigorously defined from statistical mechanics and may be calculated (with difficulty) from assumed potential forms. As expected, this equation, despite its rigorous form, is of little use in describing gases in regions where their nonideal behavior becomes very important.

The EOS in the other classes are generally semi-empirical adaptations of the results of less well-defined theoretical approaches. The cubic EOS (e.g., Redlich and Kwong, 1949) and perturbed-hard-sphere EOS (e.g., KJ EOS) are related to the van der Waal's equation, while the BWR type EOS (such as Nishiumi, 1980a, 1980b) evolved from the Beattie and Bridgeman (1928) equation through the work of Benedict et al. (1940). The corresponding EOS, typified by LK form, are based on Pitzer's corresponding state principle (1955–1958) and the BWR equation. Except for the virial EOS, which cannot be adapted to high pressure, a preferred EOS from each class was chosen as the basis of our study in this paper. The following explicit forms as well as Eqn. (1) were tested (see Section II):

1) Redlich and Kwong EOS (1949, cubic equation):

$$P = \frac{RT}{V-b} - \frac{a}{\sqrt{T}V(V+b)} \tag{A1}$$

2) Kerrick-Jacobs EOS (1981, perturbed-hard-sphere EOS):

$$P = \frac{RT(1+y+y^2-y^3)}{v(1-y^3)} - \frac{c_1 + c_2T + c_3T^2 + (d_1 + d_2T + d_3T^2)/V + (e_1 + e_2T + e_3T^2)/V^2}{\sqrt{T}V(V+b)} \tag{A2}$$

3) Benedict-Webb-Rubin EOS (1940):

$$P = RT\rho + \left(B_0RT - A_0 - \frac{Rc}{T^2}\right)\rho^2 + (bRT - a)\rho^3 + a\alpha\rho^6 + \frac{c}{t^2}\rho^3(1 + \gamma\rho^2)\exp(-\gamma\rho^2) \tag{A3}$$

4) Lee-Kesler EOS (1975):

$$\begin{aligned} Z = \Bigg[& 1 + \frac{b_{01} - b_{02}/T_r - b_{03}/T^{r^2} - b_{04}/T_r^3}{V_r} \\ & + \frac{c_{01} - c_{02}/T_r + c_{03}/T_r^3}{V_r^2} + \frac{d_{01} + d_{02}/T_r}{V_r^5} \\ & + \frac{c_{04}}{T_r^3V_r^2}\left(\beta_0 + \frac{\gamma_0}{V_r^2}\right)\exp\left(-\frac{\gamma_0}{V_r^2}\right) \\ & + \omega\Bigg(1 + \frac{b_{11} - b_{12}/T_r - b_{13}/T^{r^2} - b_{14}/T_r^3}{V_r} \\ & + \frac{c_{11} - c_{12}/T_r + c_{13}/T_r^3}{V_r^2} + \frac{d_{11} + d_{12}/T_r}{V_r^5} \\ & + \frac{c_{14}}{T_r^3V_r^2}\left(\beta_1 + \frac{\gamma_1}{V_r^2}\right)\exp\left(-\frac{\gamma_1}{V_r^2}\right)\Bigg)\Bigg] \end{aligned} \tag{A4}$$

5) Nishiumi (1980, BWR type equation):

$$\begin{aligned} Z = 1 & + \left(B_0 - \frac{A_0}{T_r} - \frac{C_0}{T_r^3} - \frac{D_0}{T_r^4} - \frac{E_0 + \Psi_E}{T_r^5}\right)\rho_r \\ & + \left(b - \frac{a}{T_r} - \frac{d}{T_r^2} - \frac{e}{T_r^5} - \frac{f}{T_r^{24}}\right)\rho_r^2 + \alpha\left(\frac{a}{T_r} + \frac{d}{T_r^2} + \frac{e}{T_r^5} + \frac{f}{T_r^{24}}\right) \\ & \times \rho_r^5\left(\frac{c}{T_r^3} + \frac{g}{T_r^9} + \frac{h}{T_r^{18}} + y(T_r)\right)\rho_r^2(1 + \gamma\rho_r^2)\exp(-\gamma\rho_r^2) \end{aligned} \tag{A5}$$

Other EOS were cited in the paper, for example, the EOS by recommended IUPAC (Angus, 1976, 1978). These equations are very complicated. Interested readers should refer to the original articles for their detailed descriptions.